

Article

# A Thermic Effect on Degradation Kinetics of Sugar Cane Bagasse Polypropylene Composites

Tshwafo E. Motaung<sup>1,2,\*</sup>, Setumo V. Motloung<sup>3,4</sup>, Lehlohonolo F. Koao<sup>5</sup>, Thembinkosi D. Malevu<sup>4</sup>  
and Ella. C. Linganiso<sup>6,7</sup>

<sup>1</sup> Department of Chemistry, School of Science in the College of Science Engineering and Technology, University of South Africa, UNISA, P.O. Box 392, Pretoria 0003, South Africa

<sup>2</sup> Department of Chemistry, Sefako Makgatho Health Science University, P.O. Box 94, Medunsa 0204, South Africa

<sup>3</sup> Department of Chemical and Physical Sciences, Mthatha Campus, Walter Sisulu University, UNITRA, Private Bag X1, Mthatha 5117, South Africa; cchataa@gmail.com

<sup>4</sup> Department of Physics, Sefako Makgatho Health Science University, P.O. Box 94, Medunsa 0204, South Africa; malevu.td@gmail.com

<sup>5</sup> Department of Physics, QwaQwa Campus, University of the Free State, Private Bag X13, Phuthaditjhaba 9866, South Africa; koaolf@ufs.ac.za

<sup>6</sup> Microscopy and Microanalysis Unit, University of the Witwatersrand, Johannesburg 2050, South Africa; linganisoella@gmail.com

<sup>7</sup> Molecular Sciences Institute, School of Chemistry, University of the Witwatersrand, Johannesburg 2050, South Africa

\* Correspondence: motaungte@live.com or motaute1@unisa.ac.za

**Abstract:** In this study, thermal degradation mechanisms and the kinetics of PP (Polypropylene) composites containing alkali and saline treated SC (Sugar cane bagasse) have been evaluated using a non-isothermal thermogravimetric analysis under consistent nitrogen atmosphere. The study indicates dynamics of kinetics that need to be considered should the composites be applied in high temperature applications. NaOH treated composites revealed a reduced fiber size compared to the other composites. The presence of SC generally reduced the functional group intensities of FTIR peaks, however some peaks re-emerged after the treatments. The composites indicated higher thermal stability and char content than the pristine polymer. In fact, NaOH treated composite is more thermally stable, while the saline is the least stable of the rest. Well known reliable degradation kinetics methods were employed in order to unpack thermal degradation behavior and possible metaphors. Flynn–Wall–Ozawa (FWO) and Kissinger–Akahira–Sunose (KAS) thermal degradation kinetic models are in agreement that the presence of both SC and those in the PP matrix that have been treated lead to increased activation energy values with the competing reactions in the degradation process. Nonetheless, the linear relation is not absolutely perfect and the competing reactions seem complex at lower temperatures as there are overlying inconsistencies in activation energies. Interestingly, bagasse indicated some effect on the mechanism that included the hindering of free radicals that emanated from the first cleavage of PP.

**Keywords:** sugar cane bagasse; thermal degradation kinetics; polypropylene composites



**Citation:** Motaung, T.E.; Motloung, S.V.; Koao, L.F.; Malevu, T.D.; Linganiso, E.C. A Thermic Effect on Degradation Kinetics of Sugar Cane Bagasse Polypropylene Composites. *J. Compos. Sci.* **2022**, *6*, 123. <https://doi.org/10.3390/jcs6050123>

Academic Editor: Francesco Tornabene

Received: 23 February 2022

Accepted: 8 April 2022

Published: 24 April 2022

**Publisher's Note:** MDPI stays neutral with regard to jurisdictional claims in published maps and institutional affiliations.



**Copyright:** © 2022 by the authors. Licensee MDPI, Basel, Switzerland. This article is an open access article distributed under the terms and conditions of the Creative Commons Attribution (CC BY) license (<https://creativecommons.org/licenses/by/4.0/>).

## 1. Introduction

Polypropylene (PP) is known for its commercial applications such as packaging, pipes, marine ropes, car interior and formation of corrugated sheets. PP is one of about 22% thermoplastics in demand across the world and the most commercially and industrially used polymer [1–5]. Its chemical resistance, durability, relatively low density and extensively high melting point have attracted a lot of attention. Nonetheless, its flammability contributes immensely when compared to the high flammability of traditional polymers applied in the industries. That has necessitated an addition of different fillers in the PP matrix,

including natural fibers. The incorporation of natural fibers, in particular, comes with series of advantages including higher stiffness, increased glass transition temperature, improved crystallinity and thermal stability of PP composites [6–11]. Sugarcane bagasse is one of the competent abundant natural fibers that has shown improved absorption, mechanical properties, viscoelastic properties and thermal properties as a filler in polypropylene. For instance, Cerqueira et al. [2] and Luz et al. [1] studied chemical modification on mechanical properties of sugarcane bagasse fiber/PP bio-composites. The presence of bagasse fiber generally exhibited a clear improvement on tensile, flexural and impact strength in comparison to the pure polymer. Modified composites have also shown interesting variations. Nevertheless, there is limited information regarding the thermal degradation kinetics of the sugarcane bagasse fiber/PP composites, especially, at low concentration of alkali.

Of late, thermal degradation kinetics of PP composites have attracted attention as its high temperature applications have expanded [12–21].

Liang et al. [15] studied thermal decomposition kinetics of polypropylene composites filled with graphene nanoplatelets using a melt blending method. The thermal degradation mechanism was a phase boundary controlled reaction (contracting volume). The activation energy increased with increasing graphene nanoplatelets lateral dimensions. A similar increase in energy was observed by Salem et al. [16] when studying the thermal degradation kinetics of virgin Polypropylene (PP) and PP with starch blends exposed to natural weathering. Nonisothermal (dynamic) thermogravimetry was used with five different heating rates. Several analytical model-free methods, including the Friedman, Achar method, Coats and Redfern, Kissinger, and Flynn–Wall–Ozawa (FWO) methods, were used for kinetic parameters. Moreover, the thermal decomposition was simulated by applying the thermal decomposition kinetics equation and the determined function parameters. Noble agreement was found between the simulations and the experimental values.

In contrast Mandal et al. [17] observed a decrease in activation energy in the addition of PLA and nanoclay in PP. They were studying thermal degradation kinetics of PP/PLA nanocomposite blends. Nonetheless, there was a noticeable increase in the  $E_a$  of the blended films in the presence of the compatibilizer. On the other hand, the lifetime of PP decreased with the addition of PLA and nanoclay. The heating rates and fractions of constituents were the main components responsible for the thermal degradation behavior and the lifetime of those that were investigated. The similar trend of observations was experienced in the investigations carried out by Vimalathithan et al. [18] and Tarani et al. [19] on graphene nanoplatelet–glass–polypropylene composites and polypropylene/clay nanocomposites, respectively.

Recorded studies have reported more on inorganic fillers and the thermal degradation kinetics of polypropylene composites. The objective of the current study is the organized comparison of the thermal degradation kinetics of SC-PP composites using the two reportedly accurate Flynn–Wall–Ozawa and Kissinger–Akahira–Sunose thermal degradation kinetic models.

## 2. Materials and Methods

### 2.1. Materials

Sugar cane bagasse (SC) was supplied by Tongaat hullet in Kwazulu Natal, South Africa, and 3-aminopropyl tri-ethoxy silane and NaOH were purchased from Sigma-Aldrich, South Africa. All chemicals were used as received without further purification. PP has a density of  $0.90 \text{ g cm}^{-3}$ , a melting point of  $165 \text{ }^\circ\text{C}$ , and an MFI of  $12 \text{ g, } 10 \text{ min}^{-1}$  and supplied by Sasol Polymers (Johannesburg, South Africa).

### 2.2. Methods

#### 2.2.1. Silane Treatment of Sugar Bagasse

A 1% solution of 3-aminopropyl tri-ethoxy silane (A1100) was prepared by mixing the silane with an ethanol/water mixture in the ratio 6/4 at PH 4 adjusted with acetic acid. The

SC was soaked in the solution for 2 h. The silane solution was drained out and the fibers were washed and dried in an oven at 70 °C until completely dry. As for NaOH treatment, dry SC was treated with an alkali solution (2 wt % NaOH) at 100 °C for 4 h before the drying step.

### 2.2.2. Extrusion of rPP with SC Fibers

A co-rotating twin-screw extruder (CTE-20, Coperion, Nanjing, China) equipped with a main feeder and side feeder as well as a strand pelletizer with a L/D ratio of 40 was employed to prepare rPP composites. SC and rPP were dried in a convection oven at 40 °C for 24 h before extrusion. The temperature during extrusion was set from 160–170 °C at a screw speed of 40 rpm.

### 2.2.3. Preparation of Composites

The injection moulding used was BOY 22M (Germany) with a 30-ton clamping force. The screw diameter was 22 mm and an L/D ratio of 30 was used to form a dumbbell of rPP/SC composites. The ratio of PP to SC for composites was kept constant at 90/10 *w/w*. The injection molding parameters are shown in Table 1.

**Table 1.** Injection molding parameters.

Barrel temperature (°C)	226
Injection speed (cm/s)	10
Injection pressure (bar)	1000
Holding pressure (bar)	150
Holding time (s)	12
Cooling time (s)	25
Shot volume (cm <sup>3</sup> )	22

## 2.3. Characterization

### 2.3.1. Scanning Electron Microscopy (SEM)

Morphology analysis of the composites were characterized by SEM. The micrographs were taken using an FEI Quanta 200 (FEI Co., Eindhoven, The Netherlands) electron microscope operated at an accelerating voltage of 15 kV. All samples were fractured in liquid nitrogen, sputter-coated with gold and allowed to dry before taking images.

### 2.3.2. Fourier Transform Infrared Spectroscopy (FTIR)

FTIR of film (1 mm) samples were carried out on a Spectrum 100 FTIR (Perkin Elmer, Waltham, MA, USA). The range used was between 500 and 4000 cm<sup>-1</sup> in ATR mode.

### 2.3.3. Thermogravimetric Analysis (TGA)

Thermogravimetric analysis was carried out with a Perkin Elmer Pyris 1 TGA. The analyses were conducted under flowing nitrogen at 20 mL·min<sup>-1</sup>, from 25–600 °C at 4 °C·min<sup>-1</sup>, 8 °C·min<sup>-1</sup>, 12 °C·min<sup>-1</sup>, and 16 °C·min<sup>-1</sup> heating rates.

## 3. Results and Discussion

### 3.1. Scanning Electron Microscope

Figure 1 displayed the SEM micrograms of PP-SC (A), PP-SC-NaOH (B) and PP-SC-silane (C). It is clear when the untreated composite (A) is compared with the rest (A and B) that there is a reduction in the cavity size adjacent to a fiber. This suggests a better compatibility of the fiber and PP with those treatments. Furthermore, the NaOH treatment seems to be more effective than the silane treatment as there is a clear reduction in the fiber size from approximately 35 µm to 20 µm compared to the untreated (A), whereas the silane treatment (C) has about 27 µm (see the arrow). These observations do not seem

strange when one examines the literature [1–5]. However, in this study, it could further be argued that the fiber dispersion is better at NaOH treatment than A and C precisely due to the fact that the surface at B appears smoother, with less fiber pull outs than A and C.

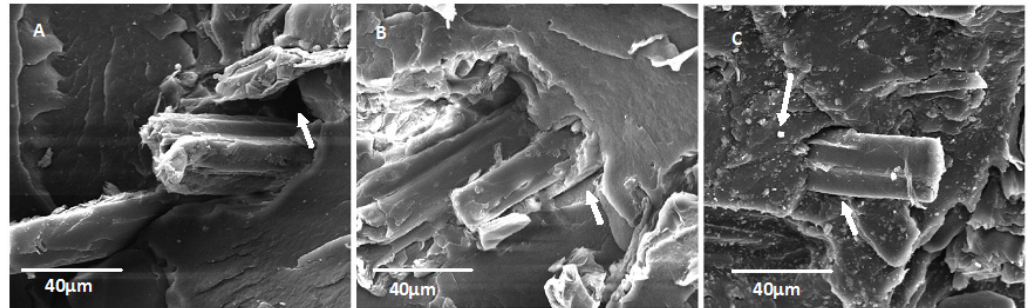


**Figure 1.** SEM of PP-SC (A), PP-SC-NaOH (B) and PP-SC-silane(C).

### 3.2. Spectral Analysis

Figure 2 shows FTIR spectra of PP, PP-SC, PP-SC-NaOH and PP-SC-silane composites.

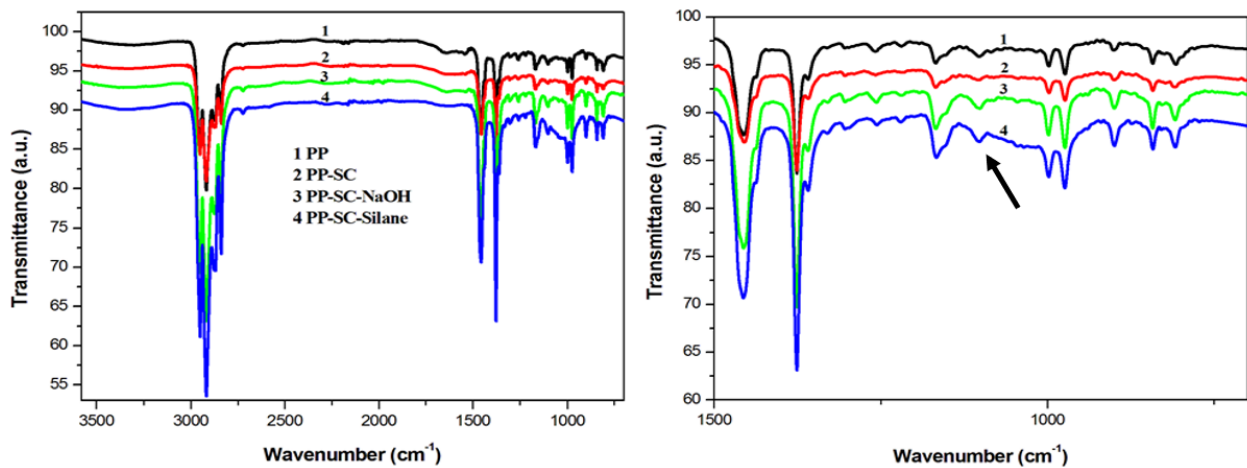


**Figure 2.** FTIR spectra of PP, PP-SC, PP-SC-NaOH and PP-SC-silane.

As expected, all the spectra displayed typical peaks of PP [20]. For example, large four peaks in wavenumber range  $3000\text{--}2800\text{ cm}^{-1}$  represent  $\text{CH}_3$  asymmetric,  $\text{CH}_3$  symmetric stretching,  $\text{CH}_2$  asymmetric and symmetric stretching vibrations, respectively, although C-C asymmetric stretching, C-H wagging and  $\text{CH}_3$  asymmetric deformation vibrations were displayed at  $1102$ ,  $1222$  and  $1258\text{ cm}^{-1}$ .

The presence of SC reduced the intensities of most peaks, pronounced from approximately  $1100$  to  $800\text{ cm}^{-1}$ . In fact, SC in PP-SC composites diminished the peaks at  $1102$ ,  $1222$  and  $1258\text{ cm}^{-1}$ , yet reappeared in the composites with treated SC. There is a broad developed peak of PP-SC-silane composite at  $1062\text{ cm}^{-1}$  related to C=C aromatic skeletal vibration of SC phenols (See an arrow). The observations are common in the literature and are mostly associated with the presence of a compatibilizer [6–10,14]. As there is no compatibilizer in the current study, the decreased intensities could be due to the reorientation of polymeric chains as the results of interfacial interaction with SC fibers, while appearance and disappearance of the peaks explain different forms of interfacial interactions owing to the surface modifications of SC. The broad peak in PP-SC-silane composite could indicate that the components in the composite have a unique interfacial interaction compared to other composites.

### 3.3. Thermal Degradation Kinetics

The degradation kinetic analysis was prepared using the following models:

### 3.3.1. Flynn–Wall–Ozawa Method (FWO)

The OFW model is an integral isoconversional method derived by using Doyle's approximation using multiple heating rates from the TGA data. The model expression is given by

$$\ln\beta = \ln AE/f(\alpha)R - 2.315 - 0.4567 E/RT \quad (1)$$

The plot of  $\ln\beta$  vs.  $1/T$  gives a straight line with a slope that is equal to  $-0.4567E/RT$ , from which activation energy can be calculated. The pre-exponential factor is calculated from the intercept of the resulting straight line by assuming a reaction model [11].

### 3.3.2. Kissinger–Akahira–Sunose Method (KAS)

From the TGA curves recorded at different heating rates  $\beta$ , temperatures  $T$  were determined at the conversions  $\alpha = 10$ –90%. The activation energies were calculated from the slope of the straight lines  $\ln(\frac{\beta}{T^2})$  versus  $\frac{1}{T}$ .

$$\ln\left(\frac{\beta}{T^2}\right) = \ln\left(\frac{AR}{E_a \cdot \alpha}\right) - \frac{E_a}{RT} \quad (2)$$

The TGA curves of the pure PP and of composites having 1.5% of untreated SC, NaOH and silane treated at a heating rate of  $10\text{ }^\circ\text{C}\cdot\text{min}^{-1}$  are reported in Figure 3. Pure PP showed a single degradation step, while all composites showed two steps degradation and an increase in char content. The first and second stages of the composites could be attributed to the SC and matrix decompositions, respectively. The increase in char content could probably be due to some cross-linked structure as the result of the interaction between the free radicals of both the PP and organic compounds of SC. The similar standard deviation values taken at  $450\text{ }^\circ\text{C}$  suggest that the SC in the polymer matrix was fairly homogeneous (Table 2). The presence of the SC in PP showed a clear increase in thermal stability. In comparison to the composite containing untreated SC, the sodium hydroxide treated SC revealed a higher thermal stability, whereas the lower stability was detected from silane treated SC composite. The effectiveness of the NaOH treatment is already corroborated by SEM results, which could place the surface area of SC at the center of TGA explanation.

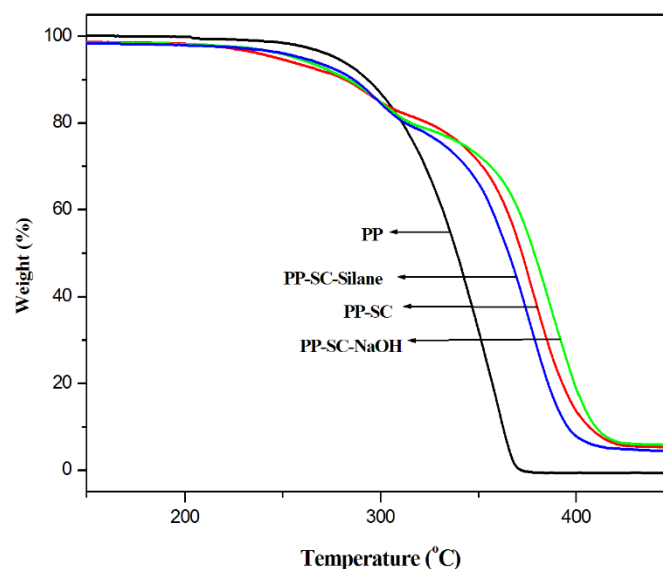


**Figure 3.** TGA curves of PP, PP-SC, PP-SC-NaOH and PP-SC-silane composites.

To get more of an insight into the thermal degradation processes, thermal degradation studies were undertaken. The most popular methods, and apparently the most accurate at determining the kinetic parameters, are the Flynn–Wall–Ozawa (FWO) and the Friedman and Kissinger–Akahira–Sunose (KAS) methods for polymer degradation [13].

Vyazovkin et al. [14] recommended the KAS method for accuracy of activation energy values. In this work the KAS and FWO methods were used. From the dynamic TGA curves of PP, PP-SC, PP-SC-NaOH and PP-SC-silane at 4, 7, 10 and 13 min<sup>-1</sup> the isoconversional graphs of lnβ versus 1/T according to Equation (1) were plotted, as well as ln(β/T<sup>2</sup>) versus 1/T according to Equation (2). The activation energy values were calculated from the slopes of the isoconversional plots. Both isoconversional methods give similar values of the activation energies within experimental uncertainty (Table 3). The graphical representation of the relationship between the activation energies and the degree of conversion are shown in Figure 4.

Table 2. Char content values for all PP-SC-composites.

Sample	Char Content/%
PP-SC	5.33 ± 0.11
PP-SC-Silane	5.10 ± 1.11
PP-SC-NaOH	6.00 ± 0.13

Table 3. Activation energy (kJ mol<sup>-1</sup>) values of thermal degradation of PP and PP-SC composite.

α	PP		PP-SC		PP-SC-NaOH		PP-SC-Silane	
	FWO	KAS	FWO	KAS	FWO	KAS	FWO	KAS
0.1	133	127	147	131	150	145	151	144
0.2	133	128	128	136	142	137	153	146
0.3	135	128	146	126	148	139	140	131
0.4	138	129	151	142	153	147	150	142
0.5	141	130	153	144	156	149	147	138
0.6	140	130	157	145	159	154	146	137
0.7	144	132	162	147	166	156	155	147
0.8	145	132	166	151	169	160	157	149
0.9	147	134	183	166	184	174	167	160

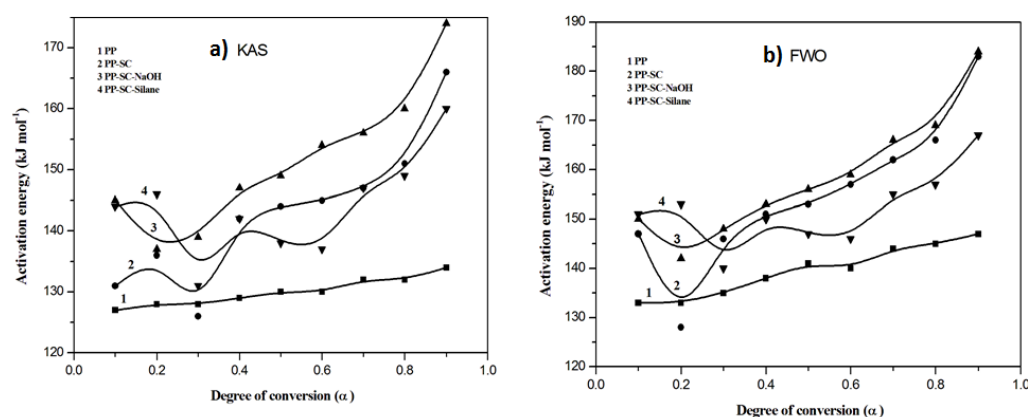
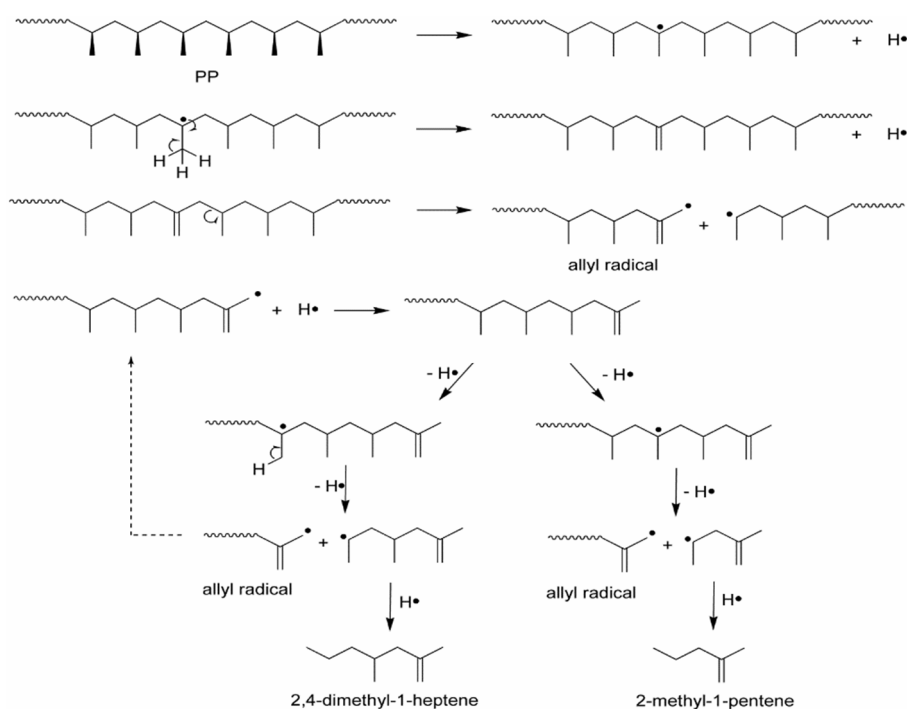


Figure 4. Activation energy values as a function of degrees of conversion obtained by (a) KAS and (b) FWO.

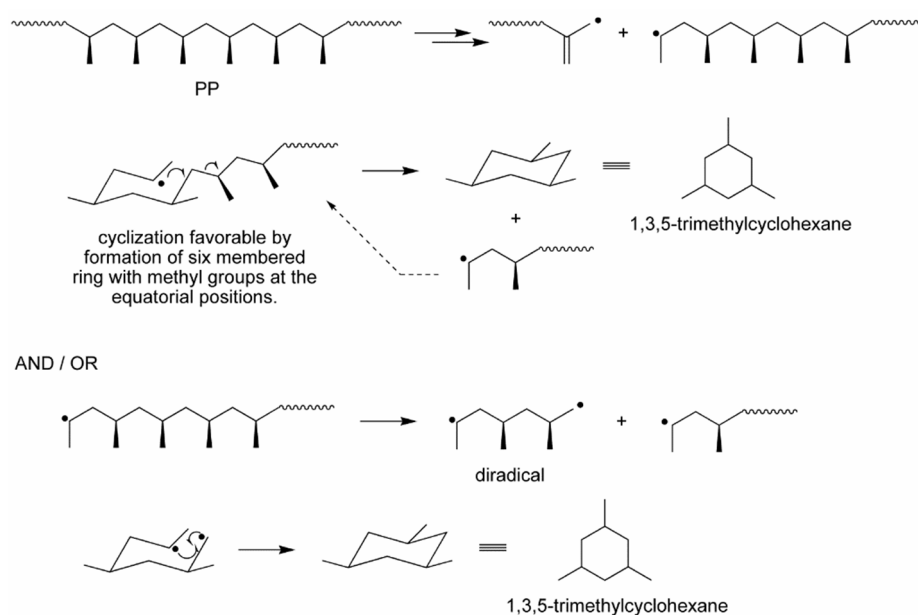
The activation energy values for the pure PP and its composite increase with the degree of conversion, however the values of PP are lower than those of the composites. The direct proportionality increase of activation energy and degree of conversion is generally related to the competing reactions in the degradation process [14]. An earlier study on the thermal degradation mechanism of PP reported that the thermal degradation of PP leads to mixture of unsaturated and saturated polymeric chains with terminated double bonds to form volatile dienes [21]. In this study that seemed to have occurred, however, the presence of a fiber hindered the process somehow by the suppression of C-C asymmetric stretching, C-H wagging and CH<sub>3</sub> asymmetric deformation vibrations.

All activation energy values match well with the literature, in which the activation energies of the thermal degradation of PP and the composites were found to range from 80 to 300 kJ mol<sup>-1</sup> [13]. The PP-SC-NaOH shows the highest activation energy followed by PP-SC values from 30% mass loss, while at lower degrees of conversion, PP-silane showed higher values of activation energy, which declined up to about 60% before increasing. Taking FTIR results into consideration, it could be suggested that C=C aromatic promoted the stability at lower temperatures. The NaOH treated SC retarded the diffusion in the volatile dienes from the PP and led to higher activation energy values than untreated SC. In the case of the silane treatment, certain intermediates seemed to have formed with an increasing  $\alpha$  that decomposed first and required a lower  $E_a$  than that of PP-SC and PP-SC-NaOH. However, at higher than 60%, it is quite possible that the char formed during the degradation of the components retarded the movement of the free radicals, which led to the observed increase in activation energy with an increase in degree of conversion.

In fact, those results seem to have logically followed Schemes 1 and 2 with regard to the thermal degradation mechanism of PP proposed by Janina et al. [12]. According to Janina et al. [12] the first cleavage of PP reportedly produced allyl and a secondary radical. The allyl radical experienced hydrogen radical addition trailed by additional cleavage, creating another allyl radical and the splinter containing the double bond that yielded 2-methyl-1-pentene and 2,4-dimethyl-1-heptene by hydrogen radical addition. Meanwhile, the secondary radical of the first cleavage suffered cyclization to a thermodynamically stable six-membered ring affording 1,3,5-trimethyl-cyclohexane and another secondary radical, which continues the same decomposition process. However, in this study the presence of fiber seemed to have interacted with dienes and alkanes after the initial cleavage to delay radicals, which clearly contributed to the increased activation energies and steeper linear relation between the activation energy and the degree of conversion. The study clarifies the importance of fiber modification in real applications in the polymer composites community and, furthermore, explains thermal degradation at the molecular level for the specified modifications.



**Scheme 1.** Proposed mechanisms for the formation of 2,4-dimethyl-1-heptene and 2-methyl-1-pentene from isotactic polypropylene degradation.



**Scheme 2.** Proposed mechanism for the formation of 1,3,5-trimethyl-cyclohexane from the isotactic polypropylene degradation.

#### 4. Conclusions

Thermal degradation and kinetics of the PP, PP composites containing alkali and silane treated SC have been successfully characterized. Furthermore, the thermal kinetic parameters relate well to the FTIR curves. SEM suggested an effective distribution of the fiber by NaOH compared to silane treatment. In fact, NaOH treatment has shown reduced fiber size compared to the silane and untreated composite. The FTIR confirmed possible interactions and bonds that led to the overlapping activation energies at lower temperatures and possible consistency at higher temperatures. The activation energy values of NaOH treated SC from Flynn–Wall–Ozawa and Kissinger–Akahira–Sunose were higher than the rest in all degrees of conversions studied. The activation energy of silane treated composite was seemingly larger than the rest at lower temperatures.

**Author Contributions:** T.E.M.: Conceptualization and write up, S.V.M., Resources, L.F.K., Resources, T.D.M., Investigation, E.C.L., Investigation. All authors have read and agreed to the published version of the manuscript.

**Funding:** No funding.

**Conflicts of Interest:** The authors declare no conflict of interest.

#### References

- Luz, S.M.; Pires, A.C.; Ferrão, P.M.C. Environmental benefits of substituting talc by sugarcane bagasse fibers as reinforcement in polypropylene composites: Ecodesign and LCA as strategy for automotive components. *Resour. Conserv. Recycl.* **2010**, *54*, 1135–1144. [[CrossRef](#)]
- Cerqueira, E.F.; Baptista, C.A.R.P.; Mulinaria, D.R. Mechanical behaviour of polypropylene reinforced sugarcane bagasse fibers composites. *Proc. Eng.* **2011**, *10*, 2046–2051. [[CrossRef](#)]
- Neto, A.G.V.C.; Ganzerli, T.A.; Cardozo, A.L.; Fávoro, S.L.; Pereira, A.G.B.; Giroto, E.M.; Radovanovic, E. Development of composites based on recycled polyethylene/sugarcane bagasse fiber. *Polym. Compos.* **2014**, *35*, 768–774. [[CrossRef](#)]
- Goulart, S.A.S.; Oliveira, T.A.; Teixeira, A.; Miléo, P.C.; Mulinari, D.R. Mechanical behaviour of polypropylene reinforced palm fibers composites. *Proc. Eng.* **2011**, *10*, 2034–2039. [[CrossRef](#)]
- Longo, C.; Savaris, M.; Zeni, M.; Brandalise, N.R.; Grisa, A.M.C. Degradation study of polypropylene (PP) and bioriented polypropylene (BOPP) in the environment. *Mater. Res.* **2011**, *14*, 442–448. [[CrossRef](#)]
- Vu, N.D.; Tran, H.T.; Nguyen, T.D. Characterization of Polypropylene Green Composites Reinforced by Cellulose Fibers Extracted from Rice Straw. *Int. J. Polym. Sci.* **2018**, *2018*, 1813847. [[CrossRef](#)]
- Shubhra, Q.T.H.; Alam, A.K.M.M.; Quaiyyum, M.A. Mechanical properties of polypropylene composites: A review. *J. Thermoplast. Compos. Mater.* **2013**, *26*, 362–391. [[CrossRef](#)]

8. Erdogan, S.; Huner, U. Physical and Mechanical Properties of PP Composites based on Different Types of Lignocellulosic Fillers. *J. Wuhan Univ. Technol.-Mater. Sci. Ed.* **2018**, *33*, 1298–1307. [[CrossRef](#)]
9. Youssef, H.A.; Ismail, M.R.; Ali, M.A.M.; Zahran, A.H. Effect of the various coupling agents on the mechanical and physical properties of thermoplastic-bagasse fiber composites. *Polym. Compos.* **2008**, *29*, 1057–1065. [[CrossRef](#)]
10. Hong, H.; Xiao, R.; Guo, Q.; Hao, L.; Zhang, H. Quantitively Characterizing the Chemical Composition of Tailored Bagasse Fiber and Its Effect on the Thermal and Mechanical Properties of Polylactic Acid-Based Composites. *Polymers* **2019**, *1567*, 1567. [[CrossRef](#)]
11. Mohomane, S.M.; Motaung, T.E.; Revaprasadu, N. Thermal Degradation Kinetics of Sugarcane Bagasse and Soft Wood Cellulose. *Materials* **2017**, *1246*, 2–12. [[CrossRef](#)] [[PubMed](#)]
12. Janina, H.B.; Rodrigo, C.; Hugo, A.G. Use of the SPME-GC-MS technique to study the thermal degradation of isotactic polypropylene: Effects of temperature and reaction time, and analysis of the reaction mechanism. *e-Polymers* **2008**, *8*, 018.
13. Chrissafis, K. Kinetics of thermal degradation of polymers. *J. Therm. Anal. Calorim.* **2009**, *95*, 273–283. [[CrossRef](#)]
14. Vyazovkin, S.; Burnham, A.K.; Criado, J.M.; Maqueda, L.A.P.; Popescu, C.; Sbirrazzuoli, N. ICTAC Kinetics Committee recommendations for performing kinetic computations on thermal analysis data. *Thermochim. Acta* **2011**, *520*, 1–19. [[CrossRef](#)]
15. Liang, J.Z.; Wang, J.Z.; Tsui, G.C.P.; Tang, C.Y. Thermal decomposition kinetics of polypropylene composites filled with graphene nanoplatelets. *Polym. Test.* **2015**, *48*, 97–103. [[CrossRef](#)]
16. Al-Salem, S.M.; Sharma, B.K.; Khan, A.R.; Arnold, J.C.; Alston, S.M.; Chandrasekaran, S.R.; Al-Dhafeeri, A.T. Thermal Degradation Kinetics of Virgin Polypropylene (PP) and PP with Starch Blends Exposed to Natural Weathering. *Ind. Eng. Chem.* **2017**, *56*, 5210–5220. [[CrossRef](#)]
17. Mandal, D.K.; Bhunia, H.; Bajpai, P.K. Thermal degradation kinetics of PP/PLA nanocomposite blends. *J. Thermoplast. Compos. Mater.* **2019**, *32*, 1714–1730. [[CrossRef](#)]
18. Vimalathithan, P.K.; Barile, C.; Casavola, C.; Arunachalam, S.; Battisti, M.G.; Friesenbichler, W.; Vijayakumar, C.T. Thermal Degradation Kinetics of Polypropylene/Clay Nanocomposites Prepared by Injection Molding Compounder. *Polym. Composites* **2019**, *40*, 3634–3643. [[CrossRef](#)]
19. Tarani, E.; Papageorgiou, G.Z.; Bikiaris, D.N.; Chrissafis, K. Kinetics of Crystallization and Thermal Degradation of an Isotactic Polypropylene Matrix Reinforced with Graphene/Glass-Fiber Filler. *Molecules* **2019**, *24*, 1984. [[CrossRef](#)]
20. Morent, R.; Geyter, N.D.; Leys, C.; Gengembre, L.; Payen, E. Comparison between XPS-and FTIT-analysis of plasma-treated polypropylene film surfaces. *Surf. Interface Anal.* **2008**, *40*, 597–600. [[CrossRef](#)]
21. Bockhorn, H.; Hornung, A.; Hornung, U.; Schawaller, D. Kinetic study on the thermal degradation of polypropylene and polyethylene. *J. Anal. Appl. Pyrolysis* **1999**, *48*, 93–109. [[CrossRef](#)]